

Constraints on electromagnetic form factors of sub-GeV dark matter from the Cosmic Microwave Background anisotropy

Gaetano Lambiase ^a, Subhendra Mohanty^b, Akhilesh Nautiyal^c and Soumya Rao^b

^a *Dipartimento di Fisica “E.R Caianiello”, Universit degli Studi di Salerno,
Via Giovanni Paolo II, 132 - 84084 Fisciano (SA), Italy*

^b *Theory Division, Physical Research Laboratory,
Navrangpura, Ahmedabad 380 009, India*

^c *Department of Physics, Malaviya National Institute
of Technology, JLN Marg, Jaipur 302017, India*

Abstract

We consider dark matter which have non-zero electromagnetic form factors like electric/magnetic dipole moments and anapole moment for fermionic dark matter and Rayleigh form factor for scalar dark matter. We consider dark matter mass $m_\chi > \mathcal{O}(\text{MeV})$ and put constraints on their mass and electromagnetic couplings from CMB and LSS observations. Fermionic dark matter with non-zero electromagnetic form factors can annihilate to e^+e^- and scalar dark matter can annihilate to 2γ at the time of recombination and distort the CMB. We analyze dark matter with multipole moments with Planck and BAO observations. We find upper bounds on anapole moment $g_A < 7.163 \times 10^3 \text{ GeV}^{-2}$, electric dipole moment $\mathcal{D} < 7.978 \times 10^{-9} \text{ e-cm}$, magnetic dipole moment $\mu < 2.959 \times 10^{-7} \mu_B$ and magnetic dipole moment for Rayleigh dark matter $\frac{g_A}{\Lambda_4^2} < 1.085 \times 10^{-2} \text{ GeV}^{-2}$ with 95% C.L.

PACS numbers: 98.80.Cq, 98.80.Ft, 26.35.+c, 95.35.+d

1. INTRODUCTION

It is well accepted that formation of large scale structures and the rotation curves of galaxies require an extra dark matter component beyond than the known particles of the standard model. The particle properties of this dark matter are, however, completely unknown. Direct detection experiments, which rely on nuclear scattering, have ruled out a large parameter space. But, these techniques are not efficient in measuring dark matter of sub-GeV mass [1]. To measure sub-GeV mass dark matter a suitable method is scattering electrons from heavy atoms [2–7]. Dark matter with non-zero electric or magnetic dipole moments [8–10] or anapole moment [11, 12] can be very effective in scattering electrons. The electromagnetic form factors can be viewed as effective operators [13–15], which arise by integrating out the heavy particles in a ultraviolet complete theory [16].

The electromagnetic couplings of dark matter can be constrained from cosmic microwave background and large scale structures observations. The electric and magnetic dipole moment vertex can give rise to dark matter-baryon coupling. For heavy dark matter (~ 100 GeV) the baryon drag on the dark matter will show up in structure formation and CMB [9]. Light dark matter ($\mathcal{O}(\text{MeV})$) will annihilate to radiation and lower the effective neutrino number (N_{eff}) [17–19].

In this paper we will analyze the effect of light dark matter with electromagnetic form factors on CMB anisotropy and polarization from dark matter annihilation to e^+e^- or photons close to recombination era, $z \sim 1100$. The effects of annihilating dark matter on CMB are studied in [20–24]. Production of relativistic e^+, e^- heats up the thermal gas and ionizes the neutral Hydrogen, which increases the free electron fraction. Due to this increased free electron fraction there is a broadening of the last scattering surface and suppression of CMB temperature anisotropy. The low- l correlations between polarization fluctuations are also enhanced due to increased freeze-out value of the ionization fraction of the universe after recombination. These effects on CMB are significant and can be used to put constraints on thermal averaged annihilation cross-section $\langle \sigma v \rangle$. Planck-2018 reports $\langle \sigma v \rangle < (3.2 \times 10^{-28}/f) \times (M_{DM}/(1\text{GeV}/c^2)) \text{cm}^3/\text{s}$ for velocity independent thermal average cross-section [25]. Here f is the fraction of energy injected to the intergalactic medium (IGM) by annihilating dark matter.

The annihilation $\chi\chi \rightarrow e^+e^-$ occur with one dipole or anapole vertex and the annihilation cross sections are quadratic in dipole or anapole moments. For fermionic dark matter the $\chi\chi \rightarrow \gamma\gamma$ annihilation cross section are quartic in dipole moments and the bounds from this process are much weaker [26] than the bounds derived from the CMB are much weaker than the ones we derive in this paper. For anapole dark matter the cross section for the process $\chi\chi \rightarrow \gamma\gamma$ is zero [11]. Scalar dark matter can have dimension-6 Rayleigh operator vertex with two-photons. For such Rayleigh dark matter the leading order contribution to annihilation will be from the $\phi\phi \rightarrow \gamma\gamma$ process which can distort the CMB near recombination and from this we put bounds on the dark-matter photon Rayleigh coupling.

This paper is organized as follows. In Section 2 we list the electromagnetic form factors of dark matter which we shall constrain from CMB data. In Section 3 we discuss the physics of recombination and the effect of dark matter annihilation on the CMB. In Section 4 we compare the CMB analysis with data from Planck and BAO and using the COSMOMC we put constraints on the dark matter form factors. In Section 5 we compare our bounds with

earlier results and give our conclusions.

2. ELECTROMAGNETIC FORM FACTORS OF DARK MATTER

Spin-1/2 dark matter can have the following electromagnetic form factors. These are the magnetic moment described by the dimension-5 operators,

$$\mathcal{L}_{\text{magnetic}} = \frac{g_1}{\Lambda_1} \bar{\chi} \sigma^{\mu\nu} \chi F_{\mu\nu} \quad (1)$$

where g_1 is a dimensionless coupling and Λ_1 is the mass scale of the particles in the loop which generate the dipole moment. The magnetic moment of Dirac fermions is $\mu = 2g_1/\Lambda_1$ and the operator (1) is zero for Majorana fermions.

Similarly electric dipole operator is of dimension-5,

$$\mathcal{L}_{\text{electric}} = \frac{g_2}{\Lambda_2} i \bar{\chi} \sigma^{\mu\nu} \gamma_5 \chi F_{\mu\nu} \quad (2)$$

where the electric dipole moment of Dirac fermions is $\mathcal{D} = 2g_2/\Lambda_2$ and the operator (2) is zero for Majorana fermions.

Finally the anapole moment is a dimension-6 operator

$$\mathcal{L}_{\text{anapole}} = \frac{g_3}{\Lambda_3^2} i \bar{\chi} \gamma^\mu \gamma_5 \chi \partial^\nu F_{\mu\nu} \quad (3)$$

This operator is non-zero for Dirac as well as Majorana fermions and the coefficient $g_A = g_3/(\Lambda_3^2)$ is called the anapole moment of χ .

Stringent bounds on sub-GeV mass dark matter are put from the observation of $\chi e^- \rightarrow \chi e^-$ scattering [2] in direct detection experiments like Xenon-10 [3], DarkSide [4] and Xenon-1T [5].

Using the experimental limits on dark matter electron scattering from Xenon-10, Xenon-1T and DarkSide bound on the electric dipole, magnetic dipole and anapole form factors of dark matter have been put in ref.[6, 7].

Real and complex scalar dark matter can have interaction with 2-photons by dimension-6 Rayleigh operator

$$\mathcal{L}_{2\phi 2\gamma} = \frac{g_4}{\Lambda_4^2} \phi^* \phi F_{\mu\nu} F^{\mu\nu} + \frac{g'_4}{\Lambda_4^2} \phi^* \phi F_{\mu\nu} \tilde{F}^{\mu\nu} \quad (4)$$

These will contribute to $\phi\phi \rightarrow \gamma\gamma$ annihilations which can be constrained from CMB [15]. In the absence of CP violation the $\tilde{F}F$ operator does not arise. The annihilation $\phi\phi \rightarrow \gamma\gamma$ takes place via s-wave in the leading order and cross section $\sigma(\phi\phi \rightarrow \gamma\gamma)v \simeq (g_4^2)m_\phi^2/\Lambda_4^4$ [15]. Bounds on the operator 4 from Xenon1T [5] and gamma ray searches from dwarf spheroidal satellites (dSphs) [27] and halo of the Milky way [28] by Fermi-LAT are obtained in ref. [15] for DM with mass larger than $\mathcal{O}(\text{GeV})$.

3. THERMAL HISTORY OF THE UNIVERSE WITH ANNIHILATING DARK MATTER

Recombination occurs around $z = 1100$ when electrons and protons combine together to form neutral hydrogen. If the annihilation cross-section of dark matter particles is sufficiently large, it can modify the history of recombination and hence can leave a clear imprint on CMB power spectrum. The shower of particles produced due to annihilation can interact with the thermal gas in three different ways. (i) The annihilation products can ionize the thermal gas, (ii) can induce Lyman- α excitation of the hydrogen that will cause more electrons in $n = 2$ state and hence increase the ionization rate and (iii) can heat the plasma. Due to the first two effects the evolution of free electron fraction χ_e changes and the last effect changes the temperature of baryons. The equation governing the evolution of ionization fraction in the presence of annihilating particles is given as

$$\frac{d\chi_e}{dt} = \frac{1}{(1+z)H(z)} [R_s(z) - I_s(z) - I_X(z)]. \quad (5)$$

Here R_s is the standard recombination rate, I_s is the ionization rate due to standard sources and I_X is the ionization rate due to annihilating dark matter particles. The computation of standard recombination rate was done in [29–31] and it is described as

$$[R_s(z) - I_s(z)] = C \times [\chi_e^2 n_H \alpha_B - \beta_B (1 - \chi_e) e^{-h_p \nu_{2s} / k_B T_b}]. \quad (6)$$

Here n_H is the number density of hydrogen nuclei, α_B and β_B are the effective recombination and photo-ionization rates for principle quantum numbers ≥ 2 in Case B recombination, ν_{2s} is the frequency of the $2s$ level from the ground state and T_b is the temperature of the baryon gas. The factor C appearing in Eqn. (6) is given by:

$$C = \frac{[1 + K \Lambda_{2s1s} n_H (1 - \chi_e)]}{[1 + K \Lambda_{2s1s} n_H (1 - \chi_e) + K \beta_B n_H (1 - \chi_e)]}. \quad (7)$$

Here Λ_{1s2s} is the decay rate of the metastable $2s$ level, $n_H (1 - \chi_e)$ is the number of neutral ground state H atoms and $K = \frac{\lambda_\alpha^3}{8\pi H(z)}$, where $H(z)$ is the Hubble expansion rate at redshift z and λ_α is the wavelength of the $Ly - \alpha$ transition from the $2p$ level to the $1s$ level.

The term I_X appearing in Eq. (5) represents the evolution of free electron density due to nonstandard sources. In our case it is due to annihilation of dark matter during recombination, which increases the ionization rate in two ways. (i) By direct ionization from the ground state and (ii) by additional $Ly - \alpha$ photons, which boosts the population at $n = 2$ increasing the the rate of photoionization by CMB. Hence, the ionization rate I_X due to dark matter annihilation is expressed as

$$I_X(z) = I_{Xi}(z) + I_{X\alpha}(z). \quad (8)$$

Here $I_{Xi}(z)$ represents the ionization rate due to ionizing photons and $I_{X\alpha}$ represents the ionization rate due to $Ly - \alpha$ photons.

The rate of energy release $\frac{dE}{dt}$ per unit volume by a relic self-annihilating dark matter particle can be expressed in terms of its thermally averaged annihilation cross-section $\langle \sigma v \rangle$

and mass m_χ as

$$\frac{dE}{dt} = 2g\rho_c^2 c^2 \Omega_{DM}^2 (1+z)^6 f(z) \frac{\langle\sigma v\rangle}{m_\chi}, \quad (9)$$

where Ω_{DM} is the dark matter density parameter, ρ_c is the critical density today, g is degeneracy factor 1/2 for Majorana fermions and 1/4 for Dirac fermions, and $f(z)$ is the fraction of energy absorbed by the CMB plasma, which is $O(1)$ factor and depends on redshift. A detailed calculation of redshift dependence of $f(z)$ for various annihilation channels is done in [23, 32–35] using generalized parameterizations or principle components. It is shown in [24, 36, 37] that the redshift dependence of $f(z)$ can be ignored up to a first approximation, since current CMB data are sensitive to energy injection over a relatively narrow range of redshift, typically $z \sim 1000 - 600$. Hence $f(z)$ can be replaced with a constant f , which we take as 1 for our analysis. Here we use 'on-the-spot' approximation, which assumes that the energy released due to dark matter annihilation is absorbed by IGM locally [22, 38, 39].

The terms appearing on the right hand side of Eq. (8) are related to the rate of energy release as

$$I_{Xi} = C\chi_i \frac{[dE/dt]}{n_H(z)E_i} \quad (10)$$

$$I_{X\alpha} = (1 - C)\chi_\alpha \frac{[dE/dt]}{n_H(z)E_\alpha}. \quad (11)$$

Here E_i is the average ionization energy per baryon, E_α is the difference in binding energy between the $1s$ and $2p$ energy levels of a hydrogen atom, n_H is the number density of Hydrogen Nuclei, and χ_i and χ_α represent the fraction of energy going ionization and $Ly-\alpha$ photons respectively; which can be expressed in terms of free electron fraction as $\chi_i = \chi_\alpha = (1 - \chi_e)/3$ [20].

A fraction of energy released by annihilating dark matter particles also goes into heating the baryon gas, which modifies the evolution equation for the matter temperature T_b by contributing one extra term K_h as

$$(1+z) \frac{dT_b}{dz} = \frac{8\sigma T a_R T_{CMB}^4}{3m_e c H(z)} \frac{\chi_e}{1 + f_{He} + \chi_e} (T_b - T_{CMB}) - \frac{2}{3k_B H(z)} \frac{k_h}{1 + f_{He} + \chi_e} + 2T_b. \quad (12)$$

Here the nonstandard term K_h arising due to annihilating dark matter is given in terms of rate of energy release as

$$K_h = \chi_h \frac{(dE/dt)}{n_H(z)}, \quad (13)$$

with $\chi_h = (1 + 2\chi_e)/3$ being the fraction of energy going into heat.

In this work we consider annihilating dark matter with electromagnetic form factors. We will now obtain the energy deposition rate for dark matter with anapole moment, electric dipole moment and magnetic dipole moment. One can define a quantity p_{ann} that depends on the properties of dark matter particles as

$$p_{ann} = f \frac{\langle\sigma v\rangle}{m_\chi}. \quad (14)$$

The current constraint on p_{ann} with velocity independent $\langle\sigma v\rangle$ is $1.795 \times 10^{-7} \text{ m}^3\text{s}^{-1}\text{kg}^{-1}$ 95% *C.L* from Planck-2018 [25]. In our analysis we will use various electromagnetic form factors and mass of the dark matter as our model parameters rather than p_{ann} . Hence we will express energy deposition rate in terms of these parameters for annihilating dark matter with anapole and dipole moments.

3.1. Dark matter with anapole moment

The annihilation cross-section for dark matter with anapole moment is given as [11],

$$\langle\sigma v\rangle_{\chi\chi\rightarrow e^+e^-} = \frac{2g_A^2\alpha m_\chi^2}{3} v_{rel}^2. \quad (15)$$

where $\alpha = e^2/(4\pi)$ and v_{rel} is average relative velocity between the annihilating dark matter particles in the centre of mass frame. The thermally averaged velocity can be expressed in terms of temperature by $\frac{1}{2}(\frac{1}{2}m_\chi)\langle v_{rel}^2 \rangle = \frac{3}{2}T$. Hence the cross-section (15) can be expressed in terms of temperature as

$$\langle\sigma v\rangle_{\chi\chi\rightarrow e^+e^-} = 4g_A^2\alpha m_\chi^2 \left(\frac{T}{m_\chi}\right). \quad (16)$$

After decoupling the temperature of the dark matter behaves as $T \propto (1+z)^2$. Assuming the decoupling temperature of the dark matter T_d of the order of $\frac{m_\chi}{10}$ we get

$$\begin{aligned} T &= T_d \frac{(1+z)^2}{(1+z_d)^2} = T_d \frac{T_0^2}{T_{\gamma d}^2} (1+z)^2 \\ &= \frac{10T_0^2}{m_\chi} (1+z)^2. \end{aligned} \quad (17)$$

Here z_d and $T_{\gamma d}$ are the redshift of dark matter decoupling and the temperature of photons at that redshift respectively, which is same as T_d . T_0 is the current temperature of CMB. Using Eq. (17) the annihilation cross-section (16) becomes

$$\langle\sigma v\rangle_{\chi\chi\rightarrow e^+e^-} = 40g_A^2\alpha T_0^2 (1+z)^2. \quad (18)$$

Hence using Eqs. (18) and (14) we can obtain the expression for p_{ann} as

$$p_{ann} = \frac{40g_A^2\alpha T_0^2}{m_\chi} (1+z)^2. \quad (19)$$

As mentioned earlier we will choose $f \sim 1$ here. Since p_{ann} is velocity dependent, the rate of energy release given by Eq. (9) will be

$$\frac{dE}{dt} = \rho_c^2 c^2 \Omega_{DM}^2 \frac{40g_A^2\alpha T_0^2}{m_\chi} (1+z)^8. \quad (20)$$

Here the redshift dependence of the energy deposition rate is modified as compared to (9).

3.2. Dark matter with electric dipole moment

For DM with electric dipole moment the annihilation cross-section is given by [10],

$$\langle\sigma v\rangle_{\chi\chi\rightarrow e^+e^-} = \frac{\alpha\mathcal{D}^2}{12}v_{rel}^2 \quad (21)$$

where v_{rel} is the relative velocity of two annihilating WIMPS. For thermal averaged cross-section $T = m_\chi \langle v_{rel}^2 \rangle / 3$. So the annihilation cross-section for dark matter can be expressed in terms of temperature as

$$\langle\sigma v\rangle_{\chi\chi\rightarrow e^+e^-} = \frac{\alpha\mathcal{D}^2}{4} \left(\frac{T}{m_\chi} \right). \quad (22)$$

Assuming $T_d \sim \frac{m_\chi}{10}$ and using Eq. (17) for temperature of the dark matter the annihilation cross-section for dark matter with electric dipole moment becomes

$$\langle\sigma v\rangle_{\chi\chi\rightarrow e^+e^-} = \frac{5\alpha\mathcal{D}^2 T_0^2}{2m_\chi^2} (1+z)^2. \quad (23)$$

Hence using (14) we get

$$p_{ann} = \frac{5\alpha\mathcal{D}^2 T_0^2}{2m_\chi^3} (1+z)^2. \quad (24)$$

In this case the energy deposition rate will be

$$\frac{dE}{dt} = \frac{1}{2} \rho_c^2 c^2 \Omega_{DM}^2 \frac{5\alpha\mathcal{D}^2 T_0^2}{2m_\chi^3} (1+z)^8. \quad (25)$$

Here also the redshift dependence is modified as compared to (9), since the thermally averaged cross-section is velocity dependent.

3.3. Dark matter with magnetic dipole moment

For dark matter with magnetic dipole moment the annihilation cross-section is given as [10],

$$\langle\sigma v\rangle_{\chi\chi\rightarrow e^+e^-} = \alpha\mu^2, \quad (26)$$

and hence

$$p_{ann} = \frac{\alpha\mu^2}{m_\chi}. \quad (27)$$

Here the annihilation cross-section does not depend on the velocity of dark matter so the energy deposition rate will be

$$\frac{dE}{dt} = \frac{1}{2} \rho_c^2 c^2 \Omega_{DM}^2 \frac{\alpha\mu^2}{m_\chi} (1+z)^6, \quad (28)$$

which has the same redshift dependence as in Eq. (9).

3.4. Rayleigh dark matter

For dark matter with magnetic dipole moment the annihilation cross-section is given by [15],

$$\langle\sigma v\rangle_{\phi\phi\rightarrow\gamma\gamma} = \frac{(g_4^2)m_\phi^2}{\Lambda_4^4}, \quad (29)$$

and hence

$$p_{ann} = \frac{(g_4^2)m_\phi}{\Lambda_4^4}. \quad (30)$$

Here again the annihilation cross-section is independent of the velocity of dark matter, so the energy deposition rate will be same as (9).

$$\frac{dE}{dt} = \frac{1}{2}\rho_c^2c^2\Omega_{DM}^2\frac{(g_4^2)m_\phi}{\Lambda_4^4}(1+z)^6. \quad (31)$$

4. CMB CONSTRAINTS ON VARIOUS MULTIPOLE MOMENTS OF DARK MATTER

As mentioned earlier annihilating dark matter increases the ionization fraction during recombination and heats the plasma. Hence the evolution equations of free electron fraction and matter temperature get modified as given by Eq. (5) and Eq. (12) respectively. The non-standard ionization rate I_X to compute free electron fraction can be obtained using Eq. (8) along with Eqs. (10) and (11). We use these equations along with energy deposition rates (20), (25), (28) and (31) for dark matter with anapole moment, electric dipole moment and magnetic dipole moment, and Rayleigh dark matter respectively to modify RECFAST routine [31] in CAMB [40]. With this we obtain modified theoretical angular power spectra, which can be used to compute the bounds on various electromagnetic form factors and mass of the dark matter from Planck-2018 data using COSMOMC [41]. The priors for the multipole moments and mass of the dark matter are given in Table I. All these priors are sampled logarithmically to cover a larger range for the new parameters. We also vary the other six parameters of Λ CDM model with priors given in [42]. We have imposed flat priors for all parameters.

Electromagnetic form factor	Priors	
Anapole	$5.0 < \ln(10^9 (g_A/GeV^{-2})) < 40$	$-3.0 < \log_{10}(m_\chi/GeV) < 2.0$
Electric dipole	$-5.0 < \ln(10^{18}(\mathcal{D}/(e - cm))) < 40$	$-3.0 < \log_{10}(m_\chi/GeV) < 2.0$
Magnetic dipole	$-10.0 < \ln(10^9(\mu/\mu_B)) < 15.0$	$-3.0 < \log_{10}(m_\chi/GeV) < 2.0$
Rayleigh dark matter	$-10.0 < \ln(10^9 g_4/(\Lambda_4^2 GeV^{-2})) < 20.0$	$-12.0 < \log_{10}(m_\chi/GeV) < 2.0$
magnetic dipole		

TABLE I: Priors on electromagnetic form factors and mass of the dark matter.

We use the lower bound for the mass of dark matter with anapole moment, and electric and magnetic dipole moment as 1 MeV since the annihilation channel for this case is $\chi\chi\rightarrow$

$e^+ e^-$. However, in case of Rayleigh dark matter with magnetic dipole moment the dark matter annihilates to photon having energy around 1 eV during recombination, which is used as the lower bound for mass of Rayleigh dark matter. We also use BAO and Pantheon data along with Planck-2018 observations for our analysis. We perform MCMC convergence diagnostic tests on 4 chains using the Gelman and Rubin "variance of mean" /"mean of chain variance" R-1 statistics for each parameter.

The constraints obtained for anapole moment and mass of the dark matter along with other six parameters of Λ CDM model are shown in Table II. Fig. 1 represents the marginalized constraints on anapole moment and mass of the dark matter along with joint 68% CL and 95% CL constraints on both the parameters from Planck-2018 and BAO data.

Parameter	68% limits	95% limits	99% limits
$\Omega_b h^2$	0.02243 ± 0.00013	$0.02243^{+0.00026}_{-0.00026}$	$0.02243^{+0.00034}_{-0.00034}$
$\Omega_c h^2$	0.11917 ± 0.00090	$0.1192^{+0.0018}_{-0.0018}$	$0.1192^{+0.0024}_{-0.0023}$
τ	0.0567 ± 0.0072	$0.057^{+0.015}_{-0.014}$	$0.057^{+0.020}_{-0.018}$
$\ln(10^9(g_A/\text{GeV}^{-2}))$	< 22.6	< 29.6	< 31.9
$\log_{10}(m_\chi/\text{GeV})$	---	---	---
$\ln(10^{10}A_s)$	3.048 ± 0.014	$3.048^{+0.029}_{-0.028}$	$3.048^{+0.039}_{-0.036}$
n_s	0.9670 ± 0.0037	$0.9670^{+0.0073}_{-0.0073}$	$0.9670^{+0.0097}_{-0.0096}$
H_0	67.73 ± 0.41	$67.73^{+0.81}_{-0.80}$	$67.7^{+1.1}_{-1.1}$

TABLE II: Planck-2018 and BAO constraints on anapole momentum and mass of the dark matter with other 6 parameters of Λ CDM

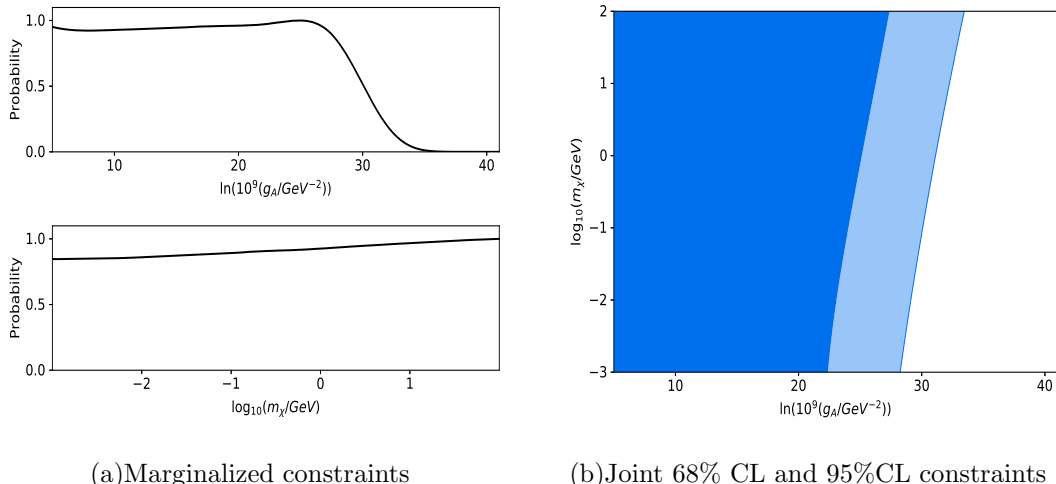


FIG. 1: Constraints for anapole moment and mass of the dark matter using Planck-2018 and BAO data

It can be seen from Table II that

$$g_A < 7.163 \times 10^3 \text{GeV}^{-2} \quad 95\% \text{C.L.} \quad (32)$$

The constraints obtained using Planck-2018 and BAO data on electric dipole moment and the mass of the dark matter along with the other six parameters of Λ CDM model are listed in Table. III. Fig. 2 depicts the marginalized constraints on electric dipole moment and mass of the dark matter and with joint 68% CL and 95%CL constraints on both the parameters from Planck-2018 and BAO data.

Parameter	68% limits	95% limits	99% limits
$\Omega_b h^2$	0.02244 ± 0.00014	$0.02244^{+0.00027}_{-0.00026}$	$0.02244^{+0.00036}_{-0.00034}$
$\Omega_c h^2$	0.11921 ± 0.00091	$0.1192^{+0.0018}_{-0.0018}$	$0.1192^{+0.0024}_{-0.0024}$
τ	0.0565 ± 0.0073	$0.056^{+0.015}_{-0.014}$	$0.056^{+0.020}_{-0.018}$
$\ln(10^{18}(\mathcal{D}/(e - cm)))$	< 12.9	< 22.8	< 26.7
$\log_{10}(m_\chi/GeV)$	> -0.963	---	---
$\ln(10^{10} A_s)$	3.048 ± 0.014	$3.048^{+0.029}_{-0.028}$	$3.048^{+0.039}_{-0.037}$
n_s	0.9670 ± 0.0037	$0.9670^{+0.0071}_{-0.0073}$	$0.9670^{+0.0093}_{-0.0097}$
H_0	67.72 ± 0.41	$67.72^{+0.82}_{-0.79}$	$67.7^{+1.1}_{-1.0}$

TABLE III: Planck-2018 and BAO constraints on electric dipole momentum and mass of the dark matter with other 6 parameters of Λ CDM

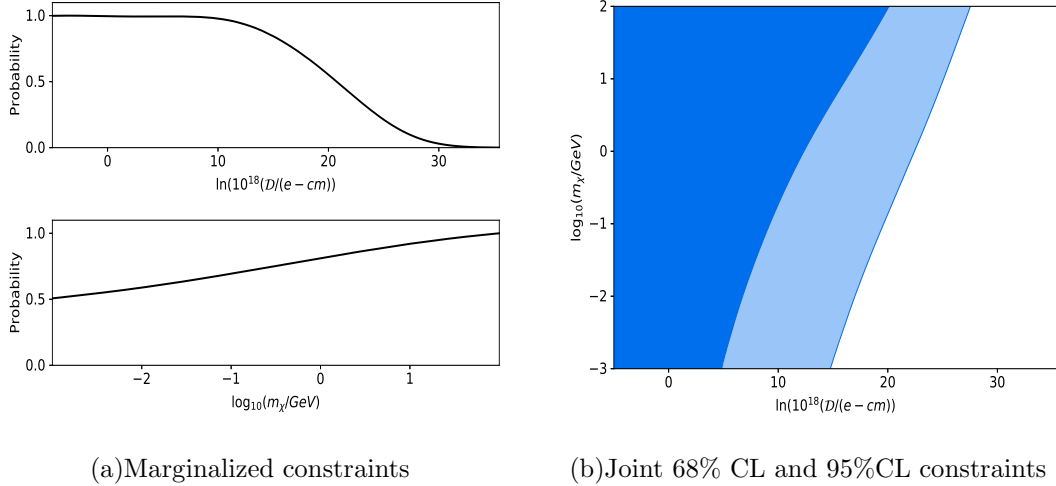


FIG. 2: Constraints for electric dipole moment and mass of the dark matter using Planck-2018 and BAO data.

We can see from Table. III that

$$\mathcal{D} < 7.978 \times 10^{-9} \text{e-cm} \quad 95\% \text{C.L.} \quad (33)$$

Table. IV represents the constraints on magnetic dipole moment and mass of the dark matter obtained from Planck-2018 and BAO data. Here also we have quoted the constraints on other six parameters of Λ CDM. Fig. 3 represents the marginalized constraints on magnetic

Parameter	68% limits	95% limits	99% limits
$\Omega_b h^2$	0.02244 ± 0.00013	$0.02244^{+0.00026}_{-0.00026}$	$0.02244^{+0.00034}_{-0.00034}$
$\Omega_c h^2$	0.11920 ± 0.00091	$0.1192^{+0.0018}_{-0.0018}$	$0.1192^{+0.0023}_{-0.0023}$
τ	0.0564 ± 0.0073	$0.056^{+0.015}_{-0.014}$	$0.056^{+0.020}_{-0.018}$
$\ln(10^9(\mu/\mu_B))$	$-2.0^{+4.0}_{-6.4}$	< 5.69	< 7.36
$\log_{10}(m_\chi/\text{GeV})$	---	---
$\ln(10^{10} A_s)$	3.047 ± 0.014	$3.047^{+0.029}_{-0.028}$	$3.047^{+0.039}_{-0.037}$
n_s	0.9671 ± 0.0037	$0.9671^{+0.0073}_{-0.0072}$	$0.9671^{+0.0096}_{-0.0093}$
H_0	67.72 ± 0.41	$67.72^{+0.82}_{-0.79}$	$67.7^{+1.1}_{-1.0}$

TABLE IV: Planck-2018 and BAO constraints on magnetic dipole momentum and mass of the dark matter with other 6 parameters of Λ CDM

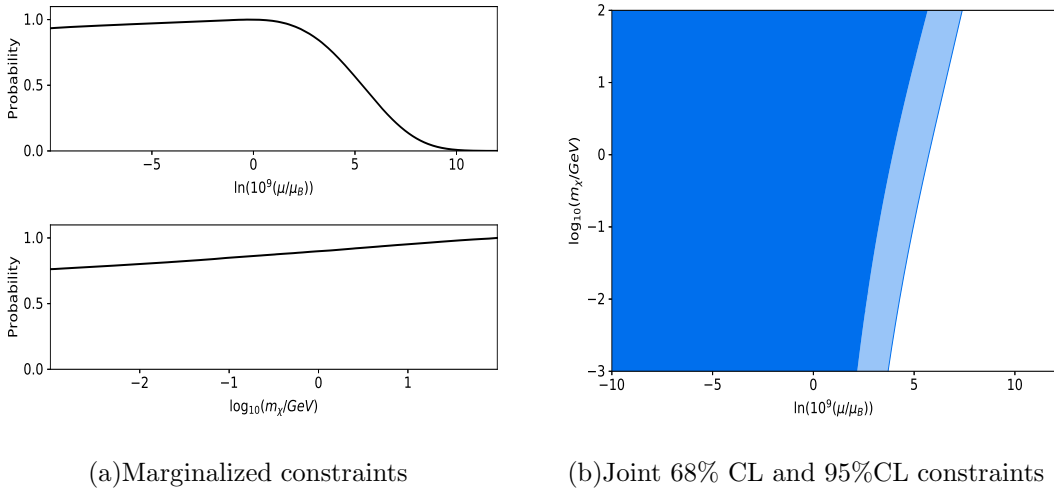


FIG. 3: Constraints for magnetic dipole moment and mass of the dark matter using Planck-2018 and BAO data.

dipole moment and mass of the dark matter along with joint 68% CL and 95%CL constraints on both the parameters.

Again we can read from Table IV that

$$\mu < 2.959 \times 10^{-7} \mu_B \quad 95\% \text{C.L.} \quad (34)$$

Similarly Table. IV lists the constraints on on magnetic dipole moment and mass of the Rayleigh dark matter. Fig. 3 represents the marginalized constraints on both of these parameters along with joint 68% CL and 95%CL constraints from Planck-2018 and BAO data. Again we have mentioned constraints on other six parameters of Λ CDM.

We can see from the Table V that

$$\frac{g_A}{\Lambda_4^2} < 1.085 \times 10^{-2} \text{ GeV}^{-2} \quad 95\% \text{C.L.} \quad (35)$$

Parameter	68% limits	95% limits	99% limits
$\Omega_b h^2$	0.02244 ± 0.00013	$0.02244^{+0.00026}_{-0.00026}$	$0.02244^{+0.00034}_{-0.00034}$
$\Omega_c h^2$	0.11919 ± 0.00092	$0.1192^{+0.0018}_{-0.0018}$	$0.1192^{+0.0023}_{-0.0024}$
τ	0.0567 ± 0.0074	$0.057^{+0.015}_{-0.014}$	$0.057^{+0.020}_{-0.019}$
$\ln(10^9 g_4 / (\Lambda_4^2 GeV^{-2}))$	< 6.43	< 16.2	< 19.7
$\log_{10}(m_\chi / GeV)$	-3.55	—	—
$\ln(10^{10} A_s)$	3.048 ± 0.015	$3.048^{+0.030}_{-0.028}$	$3.048^{+0.040}_{-0.037}$
n_s	0.9671 ± 0.0037	$0.9671^{+0.0073}_{-0.0073}$	$0.9671^{+0.0097}_{-0.0096}$
H_0	67.73 ± 0.41	$67.73^{+0.81}_{-0.80}$	
		$67.7^{+1.1}_{-1.1}$	

TABLE V: Planck-2018 and BAO constraints on magnetic dipole momentum and mass of the Rayleigh dark matter with other 6 parameters of Λ CDM

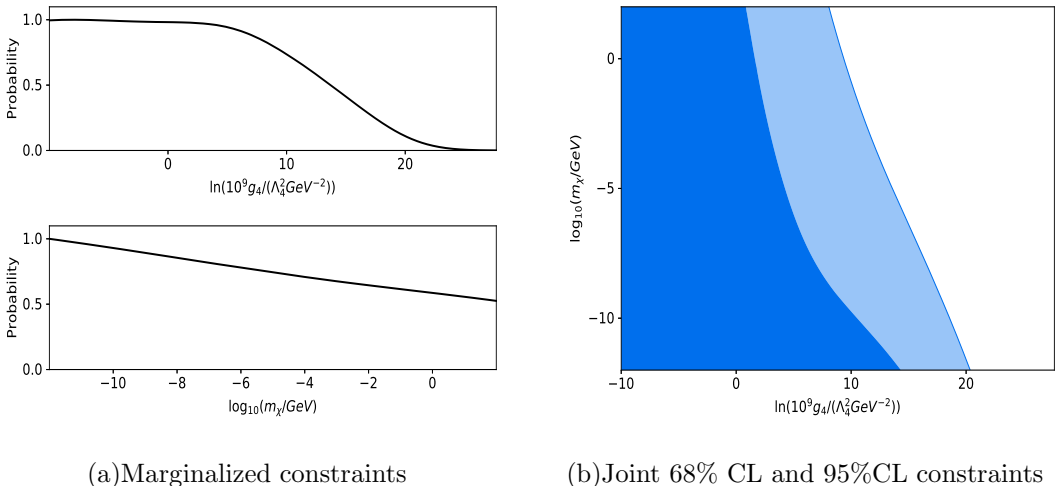


FIG. 4: Constraints for magnetic dipole moment and mass of the Rayleigh dark matter using Planck-2018 and BAO data

The upper bounds given by Eqns. (32), (33), (34) and (35) are obtained after marginalizing over all other parameters.

5. CONCLUSIONS

Electromagnetic form factors are an important class of interactions in the effective theories framework of classifying dark matter interactions. Electromagnetic dark matter can be observed but only via electron scattering direct detection experiments but can also be constrained from the CMB. Dirac fermions dark non-zero electric and magnetic dipole mo-

ments can give the correct relic density $\Omega_m h^2 = 0.11$ by the $\chi\chi \leftrightarrow f\bar{f}$ freeze-out process if $\mathcal{D} = 2.5 \times 10^{-16}$ e-cm and $\mu = 8.2 \times 10^{-7} \mu_B$ respectively [10]. Majorana fermions with anapole moment of mass 10 MeV with anapole moment $g_A = 0.11 \text{Gev}^{-2}$ can be dark matter with the correct freeze-out relic density [11].

In this paper we have considered light dark matter with masses $m_\chi > \mathcal{O}(\text{MeV})$. We find that dark matter with electromagnetic dipole or anapole form factors will distort the CMB during recombination era by producing relativistic electron via the process $\chi\chi \rightarrow e^+e^-$. We find that the Planck data gives the bounds on electromagnetic form factors $\mathcal{D} < 7.978 \times 10^{-9}$ e-cm and $\mu < 2.959 \times 10^{-7} \mu_B$, and $g_A < 7.163 \times 10^3 \text{Gev}^{-2}$ and $\frac{g_A}{\Lambda_4^2} < 1.085 \times 10^{-2} \text{GeV}^{-2}$ (95% C.L.).

Dark matter with $\mathcal{O}(\text{MeV})$ mass in thermal equilibrium with radiation will be ruled out by BBN constraints on N_{eff} . These can only have been created after the BBN era by the freeze-in mechanism. Freeze-in requires very small couplings and our bounds on electric dipole and anapole moments also rules out the freeze-out mechanism for relic density. These may be produced by the freeze-in mechanism which requires smaller couplings [45, 46].

6. ACKNOWLEDGEMENTS

A. N. would like to thank ISRO Department of Space Govt. of India to provide financial support via RESPOND programme Grant No. ISRO/RES/2/419/18-19.

- [1] T. Marrodán Undagoitia and L. Rauch, “Dark matter direct-detection experiments,” *J. Phys. G* **43**, no.1, 013001 (2016) [arXiv:1509.08767 [physics.ins-det]].
- [2] R. Essig, J. Mardon and T. Volansky, “Direct Detection of Sub-GeV Dark Matter,” *Phys. Rev. D* **85**, 076007 (2012) [arXiv:1108.5383 [hep-ph]].
- [3] R. Essig, A. Manalaysay, J. Mardon, P. Sorensen and T. Volansky, “First Direct Detection Limits on sub-GeV Dark Matter from XENON10,” *Phys. Rev. Lett.* **109**, 021301 (2012) [arXiv:1206.2644 [astro-ph.CO]].
- [4] P. Agnes *et al.* [DarkSide], “Constraints on Sub-GeV Dark-Matter–Electron Scattering from the DarkSide-50 Experiment,” *Phys. Rev. Lett.* **121**, no.11, 111303 (2018) [arXiv:1802.06998 [astro-ph.CO]].
- [5] E. Aprile *et al.* [XENON], “Light Dark Matter Search with Ionization Signals in XENON1T,” *Phys. Rev. Lett.* **123**, no.25, 251801 (2019) [arXiv:1907.11485 [hep-ex]].
- [6] R. Catena, T. Emken, N. A. Spaldin and W. Tarantino, “Atomic responses to general dark matter-electron interactions,” *Phys. Rev. Res.* **2**, no.3, 033195 (2020) [arXiv:1912.08204 [hep-ph]].
- [7] R. Catena, T. Emken and J. Ravanis, “Rejecting the Majorana nature of dark matter with electron scattering experiments,” *JCAP* **06**, 056 (2020) [arXiv:2003.04039 [hep-ph]].
- [8] M. Pospelov and T. ter Veldhuis, “Direct and indirect limits on the electromagnetic form-factors of WIMPs,” *Phys. Lett. B* **480**, 181-186 (2000) [arXiv:hep-ph/0003010 [hep-ph]].

[9] K. Sigurdson, M. Doran, A. Kurylov, R. R. Caldwell and M. Kamionkowski, “Dark-matter electric and magnetic dipole moments,” Phys. Rev. D **70**, 083501 (2004) [erratum: Phys. Rev. D **73**, 089903 (2006)] [arXiv:astro-ph/0406355 [astro-ph]].

[10] E. Masso, S. Mohanty and S. Rao, “Dipolar Dark Matter,” Phys. Rev. D **80**, 036009 (2009) [arXiv:0906.1979 [hep-ph]].

[11] C. M. Ho and R. J. Scherrer, “Anapole Dark Matter,” Phys. Lett. B **722**, 341-346 (2013) [arXiv:1211.0503 [hep-ph]].

[12] E. Del Nobile, G. B. Gelmini, P. Gondolo and J. H. Huh, “Direct detection of Light Anapole and Magnetic Dipole DM,” JCAP **06**, 002 (2014) [arXiv:1401.4508 [hep-ph]].

[13] A. De Simone and T. Jacques, “Simplified models vs. effective field theory approaches in dark matter searches,” Eur. Phys. J. C **76**, no.7, 367 (2016) [arXiv:1603.08002 [hep-ph]].

[14] X. Chu, J. Pradler and L. Semmelrock, “Light dark states with electromagnetic form factors,” Phys. Rev. D **99**, no.1, 015040 (2019) [arXiv:1811.04095 [hep-ph]].

[15] Kavanagh, B.J., Panci, P. and Ziegler, R. , Faint light from dark matter: classifying and constraining dark matter-photon effective operators. J. High Energ. Phys., **89** (2019).

[16] J. Kopp, L. Michaels and J. Smirnov, “Loopy Constraints on Leptophilic Dark Matter and Internal Bremsstrahlung,” JCAP **04**, 022 (2014) [arXiv:1401.6457 [hep-ph]].

[17] C. M. Ho and R. J. Scherrer, “Sterile Neutrinos and Light Dark Matter Save Each Other,” Phys. Rev. D **87**, no.6, 065016 (2013) [arXiv:1212.1689 [hep-ph]].

[18] C. Boehm, M. J. Dolan and C. McCabe, “A Lower Bound on the Mass of Cold Thermal Dark Matter from Planck,” JCAP **08**, 041 (2013) [arXiv:1303.6270 [hep-ph]].

[19] C. Brust, D. E. Kaplan and M. T. Walters, “New Light Species and the CMB,” JHEP **12**, 058 (2013) [arXiv:1303.5379 [hep-ph]].

[20] X. L. Chen and M. Kamionkowski, Phys. Rev. D **70**, 043502 (2004) doi:10.1103/PhysRevD.70.043502 [arXiv:astro-ph/0310473 [astro-ph]].

[21] N. Padmanabhan and D. P. Finkbeiner, Phys. Rev. D **72**, 023508 (2005) doi:10.1103/PhysRevD.72.023508 [arXiv:astro-ph/0503486 [astro-ph]].

[22] S. Galli, F. Iocco, G. Bertone and A. Melchiorri, Phys. Rev. D **80**, 023505 (2009) doi:10.1103/PhysRevD.80.023505 [arXiv:0905.0003 [astro-ph.CO]].

[23] T. R. Slatyer, N. Padmanabhan and D. P. Finkbeiner, Phys. Rev. D **80**, 043526 (2009) doi:10.1103/PhysRevD.80.043526 [arXiv:0906.1197 [astro-ph.CO]].

[24] D. P. Finkbeiner, S. Galli, T. Lin and T. R. Slatyer, Phys. Rev. D **85**, 043522 (2012) doi:10.1103/PhysRevD.85.043522 [arXiv:1109.6322 [astro-ph.CO]].

[25] N. Aghanim *et al.* [Planck], Astron. Astrophys. **641**, A6 (2020) doi:10.1051/0004-6361/201833910 [arXiv:1807.06209 [astro-ph.CO]].

[26] C. Arellano-Celiz, A. Avilez-López, J. E. Barradas-Guevara and O. Félix-Beltrán, “Annihilation of Dipolar Dark Matter to Photons,” [arXiv:1908.05695 [hep-ph]].

[27] A. Albert *et al.* [Fermi-LAT and DES], “Searching for Dark Matter Annihilation in Recently Discovered Milky Way Satellites with Fermi-LAT,” Astrophys. J. **834**, no.2, 110 (2017) [arXiv:1611.03184 [astro-ph.HE]].

[28] M. Ackermann *et al.* [Fermi-LAT], “Constraints on the Galactic Halo Dark Matter from Fermi-LAT Diffuse Measurements,” Astrophys. J. **761**, 91 (2012) [arXiv:1205.6474 [astro-ph.CO]].

[29] P. J. E. Peebles, “Recombination of the Primeval Plasma,” Astrophys. J. **153**, 1 (1968). doi:10.1086/149628

[30] Y. B. Zeldovich, V. G. Kurt and R. A. Sunyaev, “Recombination of hydrogen in the hot model of the universe,” *J. Exp. Theor. Phys.* **28**, 146 (1969) [*Zh. Eksp. Teor. Fiz.* **55**, 278 (1968)].

[31] S. Seager, D. D. Sasselov and D. Scott, “How exactly did the universe become neutral?,” *Astrophys. J. Suppl.* **128**, 407 (2000) [[astro-ph/9912182](#)].

[32] G. Huetsi, A. Hektor and M. Raidal, *Astron. Astrophys.* **505**, 999-1005 (2009) doi:[10.1051/0004-6361/200912760](#) [[arXiv:0906.4550 \[astro-ph.CO\]](#)].

[33] C. Evoli, S. Pandolfi and A. Ferrara, *Mon. Not. Roy. Astron. Soc.* **433**, 1736 (2013) doi:[10.1093/mnras/stt849](#) [[arXiv:1210.6845 \[astro-ph.CO\]](#)].

[34] S. Galli, T. R. Slatyer, M. Valdes and F. Iocco, *Phys. Rev. D* **88**, 063502 (2013) doi:[10.1103/PhysRevD.88.063502](#) [[arXiv:1306.0563 \[astro-ph.CO\]](#)].

[35] M. S. Madhavacheril, N. Sehgal and T. R. Slatyer, *Phys. Rev. D* **89**, 103508 (2014) doi:[10.1103/PhysRevD.89.103508](#) [[arXiv:1310.3815 \[astro-ph.CO\]](#)].

[36] S. Galli, F. Iocco, G. Bertone and A. Melchiorri, *Phys. Rev. D* **84**, 027302 (2011) doi:[10.1103/PhysRevD.84.027302](#) [[arXiv:1106.1528 \[astro-ph.CO\]](#)].

[37] G. Giesen, J. Lesgourgues, B. Audren and Y. Ali-Haimoud, *JCAP* **12**, 008 (2012) doi:[10.1088/1475-7516/2012/12/008](#) [[arXiv:1209.0247 \[astro-ph.CO\]](#)].

[38] L. Zhang, X. L. Chen, Y. A. Lei and Z. G. Si, *Phys. Rev. D* **74**, 103519 (2006) doi:[10.1103/PhysRevD.74.103519](#) [[arXiv:astro-ph/0603425 \[astro-ph\]](#)].

[39] L. Zhang, X. Chen, M. Kamionkowski, Z. g. Si and Z. Zheng, *Phys. Rev. D* **76**, 061301 (2007) doi:[10.1103/PhysRevD.76.061301](#) [[arXiv:0704.2444 \[astro-ph\]](#)].

[40] A. Lewis, A. Challinor and A. Lasenby, *Astrophys. J.* **538**, 473-476 (2000) doi:[10.1086/309179](#) [[arXiv:astro-ph/9911177 \[astro-ph\]](#)].

[41] A. Lewis and S. Bridle, *Phys. Rev. D* **66**, 103511 (2002) doi:[10.1103/PhysRevD.66.103511](#) [[arXiv:astro-ph/0205436 \[astro-ph\]](#)].

[42] P. A. R. Ade *et al.* [Planck], *Astron. Astrophys.* **571**, A16 (2014) doi:[10.1051/0004-6361/201321591](#) [[arXiv:1303.5076 \[astro-ph.CO\]](#)].

[43] J. Goodman, M. Ibe, A. Rajaraman, W. Shepherd, T. M. P. Tait and H. B. Yu, “Gamma Ray Line Constraints on Effective Theories of Dark Matter,” *Nucl. Phys. B* **844**, 55-68 (2011) [[arXiv:1009.0008 \[hep-ph\]](#)].

[44] P. Gondolo and K. Kadota, “Late Kinetic Decoupling of Light Magnetic Dipole Dark Matter,” *JCAP* **06**, 012 (2016) doi:[10.1088/1475-7516/2016/06/012](#) [[arXiv:1603.05783 \[hep-ph\]](#)].

[45] L. J. Hall, K. Jedamzik, J. March-Russell and S. M. West, “Freeze-In Production of FIMP Dark Matter,” *JHEP* **03**, 080 (2010) [[arXiv:0911.1120 \[hep-ph\]](#)].

[46] S. Mohanty, “Astroparticle Physics and Cosmology: Perspectives in the Multimessenger Era,” *Lect. Notes Phys.* **975**, 1-287 (2020) doi:[10.1007/978-3-030-56201-4](#)